Altering the spin state of transition metal centers in metal–organic frameworks by molecular hydrogen adsorption: A first-principles study

ARTICLE *in* PHYSICAL CHEMISTRY CHEMICAL PHYSICS · FEBRUARY 2011

Impact Factor: 4.49 · DOI: 10.1039/c0cp02373f · Source: PubMed

5 AUTHORS, INCLUDING:

Yong-Hyun Kim
Korea Advanced Institute of Science and Te…
106 PUBLICATIONS **2,884** CITATIONS
SEE PROFILE

Kyuho Lee
University of California, Berkeley
46 PUBLICATIONS **1,607** CITATIONS
SEE PROFILE

Damien West
Rensselaer Polytechnic Institute
62 PUBLICATIONS **560** CITATIONS
SEE PROFILE

PCCP

View Online
Dynamic Article Links

Cite this: *Phys. Chem. Chem. Phys.*, 2011, **13**, 5042–5046

www.rsc.org/pccp

COMMUNICATION

Altering the spin state of transition metal centers in metal–organic frameworks by molecular hydrogen adsorption: a first-principles study

Y. Y. Sun,[a] Yong-Hyun Kim,[b] Kyuho Lee,[c] D. West[a] and S. B. Zhang*[a]

Received 2nd November 2010, Accepted 19th January 2011
DOI: 10.1039/c0cp02373f

Our first-principles calculation shows that molecular hydrogen (H_2) adsorption at an exposed Fe(II) site in metal–organic frameworks could induce a spin flip in the Fe(II) center resulting in a spin-state transition from a triplet high-spin (HS) to a singlet low-spin (LS) state. The Kubas-type Fe–H_2 interaction, where H_2 coordinates onto the Fe(II) center as a σ-ligand, is found commensurate in strength with the exchange interaction of Fe 3d electrons, which is responsible for the occurrence of the spin-state transition in this system. The H_2 binding energies are 0.08 and 0.35 eV per H_2 at the HS and LS states, respectively. This effect is expected to find applications in spin-control in molecular magnets, hydrogen sensing and storage.

1. Introduction

Hydrogen molecule (H_2) could coordinate onto the transition metal (TM) centers in TM complexes without breaking the H–H bond.[1] The TM–H_2 interaction, also called Kubas interaction, is based on a mechanism of electron donation and back-donation between the TM 3d orbitals and the H_2 σ/σ* orbitals. The Kubas interaction is typically several tenths of an eV, which is comparable to the strength of the Hartree–Fock exchange interaction of the 3d electrons in a TM atom. The competition between the ligand field at the TM center, which can be modified by the H_2 adsorption, and the exchange interaction suggests the possibility that the H_2 adsorption could alter the spin state of the TM center. Such an effect could find important applications in, *e.g.*, H_2 sensing and spin-control in molecular magnets.

Spin-state transitions induced by common ligands, such as water and oxygen molecules, have been studied in bio-molecular systems, such as globins[2] and P450 enzymes,[3] for a long time. However, the H_2 molecule, as a σ-ligand, has not been widely reported to exhibit the capability to alter the spin state of TM centers except for a gas phase experiment[4] with H_2 adsorption on a $V^+(H_2)_5$ cluster, where an abnormally large adsorption energy was attributed to spin-state transition of the V^+ ion, which was later supported by a theoretical calculation.[5] For practical applications, however, it is of great interest to search for solid state materials exhibiting the effect of spin-state transition upon H_2 adsorption.

In this paper, by using first-principles calculations, we find that the effect of H_2 adsorption induced spin-state transition could occur in an Fe(II) metal–organic framework (MOF). Our calculations show that the Fe(II) centers in this material are in a triplet high-spin (HS) state, while H_2 adsorption induces a transition of the Fe(II) centers from the HS to a singlet low-spin (LS) state. The strength of the Fe–H_2 interaction is found commensurate with the exchange interaction in the Fe(II) center, which is crucial in order for the transition to occur. Indeed, the transition was not found in the same type of MOFs based on other TM elements because of a much stronger exchange interaction in those systems.

2. Computational method

Our calculations were based on the density functional theory[6,7] and Perdew–Burke–Ernzerhof approximation[8] to the exchange–correlation functional as implemented in the Vienna *Ab initio* Simulation Package (VASP).[9] All calculations were spin-polarized. The core electrons were described by the projector augmented wave potentials.[10] Plane-waves with a kinetic energy cutoff of 544 eV were used as the basis set. The Brillouin zone was represented by the Γ-point. For selected systems, calculations using (2 × 2 × 2) Monkhorst–Pack *k*-point grids[11] confirmed that the Γ-point is sufficient to give total-energy convergence to within 0.01 eV per unit cell. In all calculations, atoms were relaxed such that the forces on them are smaller than 0.01 eV $Å^{-1}$. The lattice constants were optimized by minimizing the stresses on the unit cell to less than 1 kbar. The Fe(II) MOF was calculated with its full periodic structure. The cubic unit cell contains three Fe_4Cl clusters and eight 1,3,5-benzenetristetrazolate linkers, as shown in Fig. 1a and b. In addition to the fully periodic calculations, we also adopted a smaller molecular model consisting of one Fe_4Cl cluster and eight tetrazolate rings, as shown in Fig. 1c, to facilitate electronic structure analysis of the bonding mechanism between Fe(II) centers and H_2. The dangling bonds on the eight C atoms were passivated by H. A supercell of 20 × 20 × 20 Å was used in the calculation. The use of this molecular model was justified

[a] *Department of Physics, Applied Physics, and Astronomy, Rensselaer Polytechnic Institute, Troy, New York 12180, USA. E-mail: zhangs9@rpi.edu*
[b] *Graduate School of Nanoscience and Technology (WCU) and Institute for the NanoCentury, KAIST, Daejeon 305-701, Korea*
[c] *Department of Physics and Astronomy, Rutgers University, Piscataway, New Jersey 08854, USA*

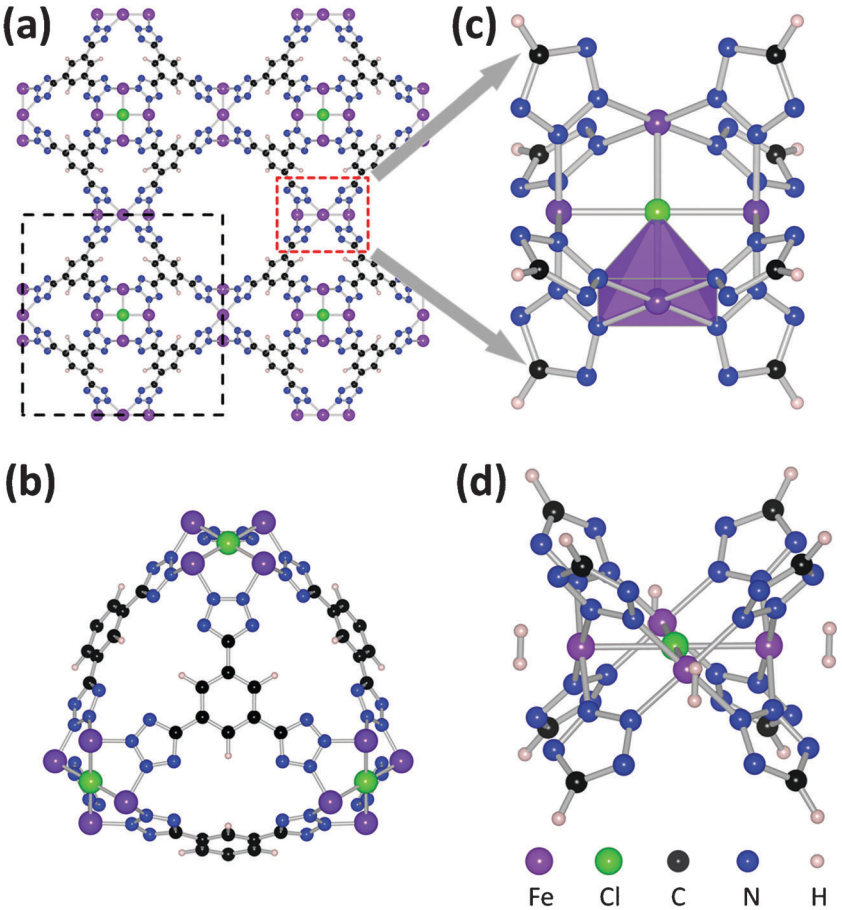

Fig. 1 (a) The unit cell of Fe(II) MOF repeated four times, viewed from the ⟨100⟩ direction. (b) A single-cell view along the ⟨111⟩ direction, showing the connection between the organic linkers and the metal clusters (Fe_4Cl). (c) The molecular model taken from the red dashed line frame in (a). The polyhedron illustrates the square pyramidal symmetry of the ligand field at an Fe site. (d) Four H_2 adsorbed at the four Fe sites in a Fe_4Cl cluster showing a side-on configuration.

Table 1 Spin magnetic moments (μ, in μ_B), binding energies of H_2 (E_b, in eV), H–H bond lengths (in Å), and Fe–H distances (in Å) obtained for high-spin (HS) and low-spin (LS) from periodic calculations with one, four and twelve H_2 per unit cell, respectively. The results from the fully loaded molecular model, as shown in Fig. 1d, are also given for comparison

	One H_2 (periodic)		Four H_2 (periodic)		Twelve H_2 (periodic)		Four H_2 (molecular)	
	HS	LS	HS	LS	HS	LS	HS	LS
μ	27	25	27	19	27	3	9	1
E_b	0.09	0.51	0.08	0.36	0.08	0.35	0.09	0.36
H–H	0.76	0.83	0.76	0.84	0.76	0.84	0.76	0.85
Fe–H	2.34	1.65	2.33	1.61	2.34	1.61	2.33	1.61

by the good agreement in structures and energetics between the molecular model and periodic calculations, as shown in Table 1.

3. Results and discussion

We investigated an Fe(II) MOF that has a structure shown in Fig. 1. Mn(II) and Cu(II) MOFs with the same structure have been recently synthesized.[12,13] The Fe(II) centers in this MOF have a nearly square pyramidal local symmetry, as shown in Fig. 1c. The ligand-field splitting of the Fe(II) 3d orbitals under this symmetry is schematically shown in Fig. 2, where the $d_{x^2-y^2}$ levels are high in energy because of steric repulsion of their four lobes with the four neighboring N atoms and, similarly, the d_{z^2} levels are higher in energy than the remaining three d orbitals because the lobe of the d_{z^2} orbital points to the Cl atom. Opposite to the effect of the ligand field, Hund's rule requires as many electrons as possible in the same spin to lower the total energy of the system by exchange interaction. Thus, there exists a competition between the exchange interaction and ligand-field splitting in the Fe(II) MOF, as reflected by the relative positions between the spin-up d_{z^2} level and the spin-down d_{xy}, d_{yz}, and d_{xz} levels (referred to as the *spin-down d_{yz} group*). If the exchange interaction is stronger than the ligand field, the spin-up d_{z^2} level is lower in energy than the spin-down d_{yz} group and a triplet HS state is obtained;

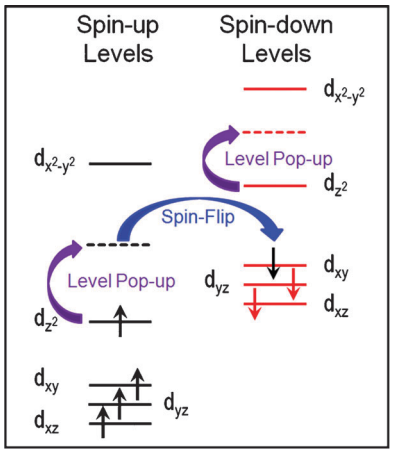

Fig. 2 Schematic illustration of the H_2 adsorption induced spin-state transition in the Fe(II) MOF. In the Fe(II) MOF, the Fe $d_{x^2-y^2}$ levels are significantly higher than all other d levels, while the d_{z^2} level is the second highest in both spin components. The ordering of d_{xy}, d_{yz} and d_{xz} levels is uncertain. But they are lower than the d_{z^2} level in both spin components. Before H_2 adsorption, the spin-up d_{z^2} level is occupied and lower than all spin-down levels so that the system stays in the high-spin state. After H_2 adsorption, due to the interaction between Fe d_{z^2} and H_2 σ, both spin-up and spin-down d_{z^2} levels are popped up to higher energies so that the spin-up d_{z^2} level becomes higher than the group of spin-down d_{xy}, d_{yz} and d_{xz} levels, which results in a spin-flip.

otherwise one level from the spin-down d_{yz} group will be occupied, which results in a singlet LS state. As the Fe(II) centers in this MOF are exposed, they are able to accommodate additional ligands, such as H_2,[12,13] which could break the established balance between the ligand field and exchange interaction. Thus, the adsorption of H_2 is potentially able to induce a spin-state transition at the Fe(II) centers.

We carried out first-principles calculations to verify the above qualitative analysis. Our calculations show that the unit cell (Fig. 1a) of the periodic Fe(II) MOF has a total spin magnetic moment of 27 μ_B, *i.e.*, 9 μ_B per Fe_4Cl cluster. The most important finding in our calculations is that, after having one H_2 adsorbed on one of the 12 Fe sites, the system at 25 μ_B has a significantly lower energy (about 0.4 eV) than that at 27 μ_B. This indicates that the H_2 adsorption induces a transition of the Fe(II) center, on which the H_2 is attached, from the HS to LS state. Calculations on additional H_2 adsorption, one by one on the other three Fe(II) centers within the same Fe_4Cl cluster, show that the total spin magnetic moment of the system is gradually reduced to 19 μ_B in 2 μ_B steps. Eventually, the H_2 adsorption proceeds to full loading with one H_2 on each of the 12 Fe(II) centers in the unit cell. In this case, the system at 3 μ_B has the lowest energy.

We calculated the H_2 binding energies according to $E_b = -[E(nH_2@MOF) - E(MOF) - n \times E(H_2)]/n$, where n is the number of adsorbed H_2, $E(H_2)$ is the total energy of an H_2 molecule in vacuum, and E(MOF) and $E(nH_2@MOF)$ are the total energies per unit cell of Fe(II) MOF without and with n adsorbed H_2, respectively. The calculated E_b for the cases with one, four, and twelve H_2 per unit cell are shown in Table 1. The stability of the LS states over the HS states after H_2 adsorption is evidenced by their higher binding energies. The strong binding at the LS states is further supported by the significantly shortened Fe–H distance and elongated H–H bond, which are also given in Table 1. At full loading of H_2, the binding energy at the LS state (0.35 eV) is comparable to those calculated on TM-decorated carbon materials for H_2 storage,[14–16] which are sufficient to hold the H_2 at room temperature. On the other hand, the binding energy at the HS state (0.08 eV) is close to pure physisorption, therefore ensures an easy desorption of H_2 at room temperature.

To understand the mechanism behind the H_2-induced spin-state transition in Fe(II) MOF, we analyzed the electronic structure of the system by employing the molecular model. Fig. 3 shows the local density of states (LDOS) for the d component of Fe and the s component of H. The orbital characteristics of the peaks in the LDOS are identified by examining the partial charge densities due to individual molecular orbitals. Examples of the partial charge densities, characteristics of the d_{z^2} and d_{yz} orbitals, are given in Fig. 4. For Fe, the positions of the d_{z^2} levels are marked by (*) in Fig. 3. It can be seen that, before H_2 adsorption, the spin-up d_{z^2} orbitals are all occupied, while after H_2 adsorption, they become depopulated. Upon H_2 adsorption, the spin-up d_{z^2} levels are pushed to a position higher than those of the spin-down d_{yz} group due to the interaction between Fe d_{z^2} and H_2 σ orbitals. Thus, the electron originally occupying the spin-up d_{z^2} level is transferred to one of the spin-down levels, which corresponds to a change in spin magnetic moment of 2 μ_B. Fig. 2 shows a schematic illustration of the spin-flip process, which is consistent with the qualitative analysis made above.

To gain insight into the nature of the Fe–H_2 bonding, we further analyzed the molecular orbitals. The bonding mechanism was found to be the same as that in the Kubas complexes,[1] where the interaction between the TM center and the H_2 σ-ligand is explained based on a donation and back-donation picture. It is worthwhile to note that the electron back-donation channel determines the orientation of

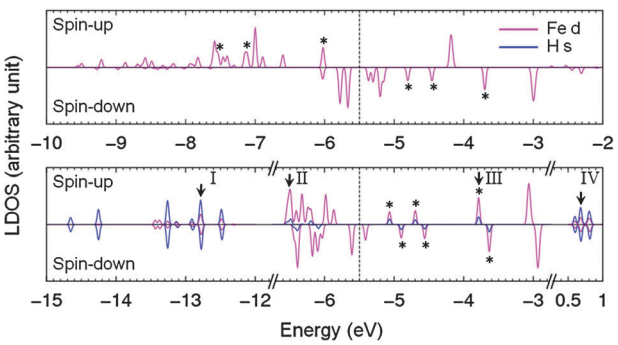

Fig. 3 Local density of states (LDOS). The upper panel is for the case before H_2 adsorption, where the system is in the HS state. Only the d component of Fe is shown in this case. The lower panel is for the case after H_2 adsorption, where the system is in the LS state. Both the d component of Fe and the s component of H are shown in the lower panel. The d_{z^2} levels are marked by (*). The dashed lines separate the occupied and unoccupied states. Arrows and the accompanying roman numerals mark the hybridization orbitals between Fe and H_2, which are shown in Fig. 4. Note that, in the lower panel, the abscissa is segmented showing three relevant regions.

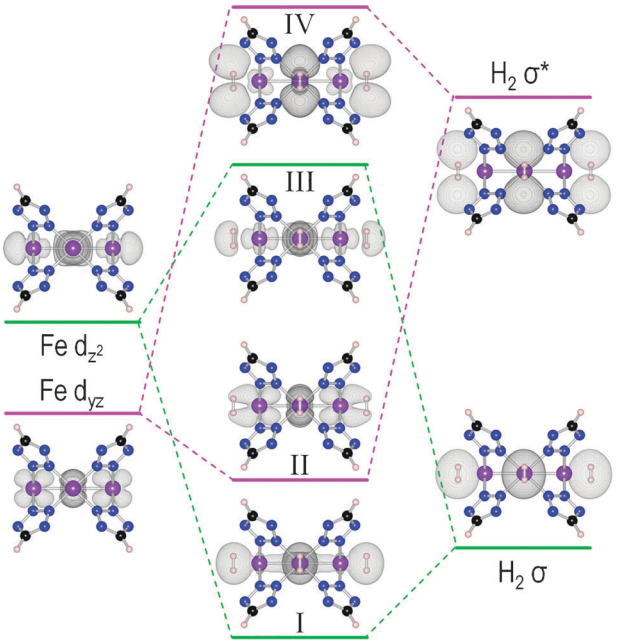

Fig. 4 Orbital interaction diagram for Fe d and H_2 together with the calculated molecular orbitals before and after hybridization. The green lines show the donation process from H_2 σ to Fe d_{z^2}. The pink lines are for the back-donation from Fe d_{yz} to H_2 σ*. The orbitals I and II are the bonding states for donation and back-donation processes, respectively. Similarly, the orbitals III and IV are the anti-bonding states.

the adsorbed H_2, *i.e.*, the side-on configuration as shown in Fig. 1d, which is also the configuration determined by neutron diffraction experiments.[12,13] Fig. 4 identifies the bonding and anti-bonding states corresponding to both the donation and back-donation channels in the Fe–H_2 bonding. The donation of electron from H_2 to Fe happens through the interaction (or hybridization) between H_2 σ and Fe d_{z^2}, while the back-donation is between Fe d_{yz} and H_2 σ*. Orbital plots II and IV in Fig. 4 further confirm that the orientation of the adsorbed H_2 is indeed determined by the electron back-donation (*i.e.*, by hybridization between Fe d_{yz} and H_2 σ*).

In contrast to the case of Fe(II) MOF, the H_2 induced spin-state transition was not found in Cr(II) and Mn(II) MOFs having the same structure.[17] We attribute this to the weaker exchange interaction in Fe(II) than in Cr(II) and Mn(II). The strength of the exchange interaction is reflected in the total-energy difference between the HS and LS states (ΔE_{HS-LS}) of the system before H_2 adsorption. Our calculations give $\Delta E_{HS-LS} = -1.03$, -0.83 and -0.36 eV per TM atom in Cr(II), Mn(II) and Fe(II) MOFs, respectively. This indicates that, before the H_2 adsorption, the HS state is always more stable than the LS state. However, this stability is more pronounced in Cr(II) and Mn(II) MOFs, and accordingly, it requires a larger ligand-field splitting of the d orbitals, which is more difficult, to induce spin-state transition for the Cr(II) and Mn(II) MOFs.

4. Conclusion

We have demonstrated that molecular H_2 adsorption can induce a change in magnetic properties of solid-state materials, specifically, a spin-state transition of the Fe(II) centers in a Fe(II) MOF. The interaction between the H_2 σ and Fe d_{z^2} orbitals is found to be the origin of this effect. By identifying the donation and back-donation channels between the Fe(II) center and the H_2 σ-ligand, we conclude that the bonding mechanism here is the same as that in Kubas complexes. The weaker exchange interaction in the Fe(II) center compared with the Cr(II) and Mn(II) centers in similar MOFs is the key to the spin-state transition in the Fe(II) MOF. Such an effect could be used for H_2 sensing as well as spin-control in porous and molecular magnets for quantum computing. In addition, it has been well known that light irradiation can also induce spin-state transition in the TM centers.[18–21] This offers a novel mechanism for H_2 storage, *i.e.*, non-thermal control on H_2 uptake and release, which could avoid the temperature related issues in current storage materials.[22,23]

Acknowledgements

Calculations of this work were done at Computational Center for Nanotechnology Innovations (CCNI) of Rensselaer Polytechnic Institute. This work was supported by DOE/OS/BES and DOE/EERE through the Hydrogen Sorption Center of Excellence under Grant No. DE-AC36-08GO28308 and Subcontract to RPI No. J30546 and J90336. Y.-H.K. was supported by WCU (World Class University) program through the National Research Foundation of Korea (R31-2008-000-10071-0) and KAIST Institute program (N10100041).

References

1 G. J. Kubas, Fundamentals of H_2 Binding and Reactivity on Transition Metals Underlying Hydrogenase Function and H_2 Production and Storage, *Chem. Rev.*, 2007, **107**, 4152–4205.
2 J. P. Collman, R. Boulatov, C. J. Sunderland and L. Fu, Functional Analogues of Cytochrome *c* Oxidase, Myoglobin, and Hemoglobin, *Chem. Rev.*, 2004, **104**, 561–588.
3 S. Shaik, D. Kumar, S. P. de Visser, A. Altun and W. Thiel, Theoretical Perspective on the Structure and Mechanism of Cytochrome P450 Enzymes, *Chem. Rev.*, 2005, **105**, 2279–2328.
4 J. E. Bushnell, P. R. Kemper and M. T. Bowers, Spin Change Induced in Vanadium(I) by Low-Field Ligands: Binding Energies of $V+(H_2)_n$ Clusters (n = 1–7), *J. Phys. Chem.*, 1993, **97**, 11628–11634.
5 P. Maitre and C. W. Bauschlicher, Jr., Structure of $V(H_2)_n^+$ Clusters for n = 1–6, *J. Phys. Chem.*, 1995, **99**, 6836–6841.
6 P. Hohenberg and W. Kohn, Inhomogeneous Electron Gas, *Phys. Rev.*, 1964, **136**, B864–B871.
7 W. Kohn and L. J. Sham, Self-Consistent Equations Including Exchange and Correlation Effects, *Phys. Rev.*, 1965, **140**, A1133–A1138.
8 J. P. Perdew, K. Burke and M. Ernzerhof, Generalized Gradient Approximation Made Simple, *Phys. Rev. Lett.*, 1996, **77**, 3865–3868.
9 G. Kresse and J. Furthmüller, Efficiency of *Ab initio* Total Energy Calculations for Metals and Semiconductors Using a Plane-wave Basis Set, *Comput. Mater. Sci.*, 1996, **6**, 15–50.
10 G. Kresse and D. Joubert, From Ultrasoft Pseudopotentials to the Projector Augmented-wave Method, *Phys. Rev. B: Condens. Matter Mater. Phys.*, 1999, **59**, 1758–1775.
11 H. J. Monkhorst and J. D. Pack, Special Points for Brillouin-Zone Integrations, *Phys. Rev. B: Solid State*, 1976, **13**, 5188–5192.
12 M. Dincă, A. Dailly, Y. Liu, C. M. Brown, D. A. Neumann and J. R. Long, Hydrogen Storage in a Microporous Metal-Organic Framework with Exposed Mn^{2+} Coordination Sites, *J. Am. Chem. Soc.*, 2006, **128**, 16876–16883.
13 M. Dincă, W. S. Han, Y. Liu, A. Dailly, C. M. Brown and J. R. Long, Observation of Cu^{2+}-H_2 Interactions in a Fully

Desolvated Sodalite-Type Metal-Organic Framework, *Angew. Chem., Int. Ed.*, 2007, **46**, 1419–1422.
14 Y. Zhao, Y.-H. Kim, A. C. Dillon, M. J. Heben and S. B. Zhang, Hydrogen Storage in Novel Organometallic Buckyballs, *Phys. Rev. Lett.*, 2005, **94**, 155504.
15 T. Yildirim and S. Ciraci, Titanium-Decorated Carbon Nanotubes as a Potential High-Capacity Hydrogen Storage Medium, *Phys. Rev. Lett.*, 2005, **94**, 175501.
16 H. Lee, W. I. Choi and J. Ihm, Combinatorial Search for Optimal Hydrogen-Storage Nanomaterials Based on Polymers, *Phys. Rev. Lett.*, 2006, **97**, 056104.
17 Y. Y. Sun, Y.-H. Kim and S. B. Zhang, Effect of Spin State on the Dihydrogen Binding Strength to Transition Metal Centers in Metal-Organic Frameworks, *J. Am. Chem. Soc.*, 2007, **129**, 12606–12607.
18 P. Gütlich, A. Hauser and H. Spiering, Thermal and Optical Switching of Iron(II) Complexes, *Angew. Chem., Int. Ed. Engl.*, 1994, **33**, 2024–2054.
19 O. Kahn and C. J. Martinez, Spin-Transition Polymers: from Molecular Materials toward Memory Devices, *Science*, 1998, **279**, 44–48.
20 S. Decurtins, P. Gütlich, C. P. Köhler, H. Spiering and A. Hauser, Light-Induced Excited Spin State Trapping in a Transition-Metal Complex: The Hexa-1-Propyltetrazole-Iron(II) Tetrafluoroborate Spin-Crossover System, *Chem. Phys. Lett.*, 1984, **105**, 1–4.
21 C. Bressler, C. Milne, V.-T. Pham, A. ElNahhas, R. M. van der Veen, W. Gawelda, S. Johnson, P. Beaud, D. Grolimund, M. Kaiser, N. C. Borca, G. Ingold, R. Abela and M. Chergui, Femtosecond XANES Study of the Light-Induced Spin Crossover Dynamics in an Iron(II) Complex, *Science*, 2009, **323**, 489–492.
22 L. Schlapbach and A. Züttel, Hydrogen-Storage Materials for Mobile Applications, *Nature*, 2001, **414**, 353–358.
23 U. Eberle, M. Felderhoff and F. Schüth, Chemical and Physical Solutions for Hydrogen Storage, *Angew. Chem., Int. Ed.*, 2009, **48**, 6608–6630.

